0026-895X/96/010052-08$3.00/0

MOLECULAR PHARMACOLOGY, 50:52–59 (1996).

Bimodal Distribution of Renal Cytochrome P450 3A Activity in Humans

BARBARA D. HAEHNER, J. CHRISTOPHER GORSKI, MARK VANDENBRANDEN, STEVEN A. WRIGHTON, SRINIVAS K. JANARDAN, PAUL B. WATKINS, and STEPHEN D. HALL

Department of Medicine, Indiana University School of Medicine, Indianapolis, Indiana 46202 (B.D.H., J.C.G., S.D.H.), Department of Drug Metabolism, Lilly Research Laboratories, Indianapolis, Indiana 46285 (M.V., S.A.W), and Department of Medicine, University of Michigan Medical Center, Ann Arbor, Michigan 48109 (S.K.J., P.B.W.)

Received December 21, 1995; Accepted April 5, 1996

SUMMARY

It has been proposed that excessive intrarenal conversion of cortisol to 6β-hydroxycortisol by CYP3A may mediate increased tubular reabsorption of sodium, leading to a state of mild volume expansion and the clinical phenotype of salt-sensitive hypertension. Therefore, we characterized CYP3A activity in a bank of microsomes from human kidneys using the formation of 1′-hydroxymidazolam (1′-OHM) as a prototypical CYP3A-catalyzed reaction. Maximal rates of metabolite formation occurred at midazolam concentrations of 12.5–50 μM; higher concentrations resulted in dramatic substrate inhibition. At 12.5 μM midazolam, 4 of 27 kidneys exhibited relatively high mean ± standard deviation 1′-OHM formation rate (184.0 ± 14.4 pmol/hr/mg) compared with the remaining 23 samples, which had a mean formation rate of (10.1 ± 6.4 pmol/hr/mg). Triacetyloleandomycin and anti-CYP3A antibody inhibited midazolam hydroxylation by 53% and 57%, respectively. The correlation between CYP3A5 content, determined through immunoblotting, and 1′-OHM formation rate was high (r^2 = 0.84, 24 experiments). The expressions of mRNA corresponding to *CYP3A3*, *CYP3A4*, *CYP3A5*, and *CYP3A7* were determined through polymerase chain reaction with specific oligonucleotides as primers. All kidneys examined (25 experiments) expressed CYP3A5 protein and contained the corresponding CYP3A5 mRNA. CYP3A4 mRNA was detected in 40% of the kidney samples, and 70% of those that contained detectable CYP3A4 mRNA also expressed detectable levels of the corresponding protein. Therefore, in contrast to hepatic tissue, in which CYP3A4 is universally expressed, CYP3A5 is the ubiquitously expressed member of the *CYP3A* family in renal tissue. The distribution of enzyme activity and protein content suggests bimodality and may represent induction of *CYP3A5* in a select population and/or a genetically determined organ-specific pattern of expression.

Intrarenally produced products generated by CYP seem to play a role in integrated renal function by altering ion transport and regional vasoactivity. The intrarenally CYP-generated products of arachidonic acid, derived primarily from enzymes in the *CYP2C* and *CYP4A* subfamilies, have been well characterized with respect to these activities (1). It has been previously noted in a small number of immunoblotted human kidney microsomal samples that CYP3A5 was expressed in five of seven samples, whereas CYP3A4 was expressed in only 14% of samples (2). Based on immunohistochemical studies of the human kidney, CYP3A seems to be located in the proximal tubule, thin limb of Henle, the cortical collecting ducts, and the cells lining the renal pelvis (3). However, the role of CYP3A in renal physiology and/or pathophysiology has been less well characterized than that of CYP2C and CYP4A. It has been established that both human CYP3A4 (4) and CYP3A5 (5) catalyze the conversion of cortisol to its 6β-hydroxy metabolite. Consequently, a pathophysiological role of renal CYP3A has been suggested to occur as a result of excessive intrarenal conversion of cortisol to 6β-OHC. Increased levels of 6β-OHC in the renal tubule may mediate enhanced sodium reabsorption via a unique nuclear receptor, which, in turn, could result in a clinical picture of salt-sensitive hypertension (6–8). Cushing's syndrome, estrogen administration, and preeclampsia are human conditions that are associated with both hypertension and excessive urinary excretion of 6β-OHC. In addition, salt-sensitive African-Americans with hypertension also may have increased urinary 6β-OHC/cortisol ratios (8).

From studies with SHR, increased levels of renal CYP3A

This work was supported in part by a Department of Veterans Affairs fellowship (B.D.H.) and by National Institutes of Health Grants T32-GM08425 and PO1-ES04238.

ABBREVIATIONS: CYP, cytochrome P450; SHR, spontaneously hypertensive rats; 6β-OHC, 6β-hydroxycortisol; MDZ, midazolam; 1′-OHM, 1′-hydroxymidazolam; 4-OHM, 4-hydroxymidazolam; PCR, polymerase chain reaction; IUK, IU kidney; NTV, normal test variable; HL-A, human hepatic microsomes with CYP3A4; HL-E, human hepatic microsomes with CYP3A4 and CYP3A5; HPLC, high performance liquid chromatography.

have been linked with increased production of 6β-hydroxycorticosterone (rat endogenous glucocorticoid) and systemic hypertension (9). The SHR exhibit a 6-fold increase in renal CYP, systemic hypertension, and increased urinary excretion of 6β-hydroxycorticosterone relative to normotensive Wistar-Kyoto rats (9, 10). The nonspecific destruction of renal CYP with stannous chloride (11) and the more specific inhibition of CYP3A with triacetyloleandomycin resulted in decreased 6β-hydroxycorticosterone excretion and significantly lower blood pressure in SHR (9). This animal model therefore provides a direct link among increased intrarenal levels of CYP3A, hypertension, and the increased formation of 6β-hydroxycorticosterone. Therefore, in view of the putative importance of renal CYP3A, we set out to characterize the variability of CYP3A catalytic activity in a large group of human renal microsomes with MDZ as a prototypical CYP3A substrate and to examine the variability of CYP3A protein expression through immunoblot analysis. We used CYP-specific PCR to detect the presence of CYP3A mRNA message in the corresponding human renal tissue.

Materials and Methods

Tissue samples. After approval by the Institutional Review Board of Indiana University Hospital, human renal tissue was obtained from patients undergoing total or partial nephrectomy primarily for renal cell carcinoma, transitional carcinoma, or testicular carcinoma. Two organs were harvested donor kidneys that were not transplanted. Tissue was rinsed in phosphate-buffered saline within 60–90 min of surgical removal, cut into 0.5-cm cubes, frozen in liquid nitrogen, and stored at −70°. Twenty-nine kidney samples were obtained, of which 24 had normal cortex/medulla, whereas 5 had moderate to severe cortical thinning, scarring, or both. The age of the population ranged from 14 to 79 years, with a median age of 46.

Microsome preparation. Frozen human renal tissue was homogenized in 0.05 M Tris·HCl, pH 7.4, containing 0.15 M potassium chloride, 1 mM EDTA, 1 mM dithiothreitol, and 0.1 mM phenylmethylsulfonyl fluoride, and microsomes were prepared with the use of differential centrifugation as described previously (12). The 100,000 × *g* pellet (microsomal fraction) was resuspended in 0.1 M tetrapotassium pyrophosphate, pH 7.4, with 0.15 M potassium chloride, 1 mM dithiothreitol, and 0.1 mM phenylmethylsulfonyl fluoride and washed in a second 100,000 × *g* centrifugation. The pellet was resuspended in a final buffer consisting of 100 mM sodium phosphate buffer, pH 7.4, containing 1 mM EDTA, 20% glycerol, and 1 mM dithiothreitol and stored at −70°. Final microsomal protein concentrations, determined according to the Lowry method (13), ranged from 7 to 50 μg/μl.

Microsomal incubations. MDZ required purification before use as a microsomal substrate because small amounts of 1′-OHM and 4-OHM were present in the unpurified material. Purification was effected through HPLC with a semipreparative C-18 column (5 μm × 10 mm × 250 cm Ultrasphere; Beckman Instruments, Palo Alto, CA), a mobile phase consisting of methanol/potassium phosphate (100 mM, pH 7.4)/tetrahydrofuran (60:38:2) eluted at a rate of 3 ml/min, and detected with ultraviolet absorbance at 230 nm. The well-resolved peak corresponding to MDZ, which eluted at 15 min, was collected, evaporated, and reconstituted with methanol, and the concentration was determined spectrophotometrically through UV absorbance.

Microsomal incubations were performed in duplicate as described previously (14) and contained a final concentration of 100 mM sodium phosphate, pH 7.4, 5 mM isocitrate, 0.1 mM EDTA, isocitrate dehydrogenase (1 unit), and 1.0 mg of human kidney microsomal protein in a total reaction volume of 800 μl. To initiate the reaction, 1 mM NADPH with 5 mM magnesium chloride was added to the system, which was then incubated for 1 hr at 37°. The reaction was terminated by adding 100 μl of 0.3 M barium hydroxide, 100 μl of 0.3 M zinc sulfate, 400 μl of ice-cold ethyl acetate, and 200 μl of $^{15}N_3$-1′-OHM (stable isotope) (internal standard). The rate of 1′-OHM formation was linear with time up to 2 hr under these conditions. Control incubations were identical to those above except that the incubation time was zero or microsomal protein was omitted. Potential inhibition by triacetyloleandomycin was examined at 100 μM and preincubated for 30 min with NADPH, followed by the addition of 12.5 μM MDZ. Inhibition with antibody was examined with a rabbit anti-CYP3A4 antibody that has previously shown to be inhibitory and to recognize only CYP3A proteins (15). The volume of antibody used was based on relative catalytic activity compared with the volumes used to inhibit hepatic microsomal CYP3A activity; volumes of 0.5, 1.0, and 10 μl of the antisera were used. Anti-CYP3A antibody or preimmune serum was preincubated with microsomal protein for 30 min, after which NADPH, magnesium chloride, and 12.5 μM MDZ were added as described above.

MDZ metabolite analysis. Microsomal incubation mixtures and quality controls (3–100 ng of metabolite plus rat kidney homogenate but no NADPH) were extracted twice with 2.5 ml of ethyl acetate, and the organic layer was decanted, dried under nitrogen, and reconstituted with 75 μl of mobile phase (*vide infra*). The peaks corresponding to 1′-OHM and 4-OHM were collected from an HPLC equipped with a C-18 column (5 μm × 2.6 mm × 25 cm, Ultrasphere, Beckman Instruments) and eluted with the mobile phase methanol/potassium phosphate (100 mM pH 7.4)/tetrahydrofuran (52:46:2) flowing at 1 ml/min. The collected peaks were partially dried in a rotary evaporator and extracted twice with 3 ml ethyl acetate, and the organic layer was decanted. The organic phase was then evaporated to dryness under nitrogen. The samples were then reconstituted with 150 μl of methanol, placed into gas chromatography-mass spectrometry vials, and reconcentrated in a rotary evaporator. These sample residues were derivatized in 20–100 μl of *N*-methyl-*N*-trimethyl-silyl-trifluoroacetamide (Pierce, Rockford, IL) by heating to 70° for 15 min and then injected onto a Hewlett Packard 5971A gas chromatography-mass spectrometry. The gas chromatography column was an HP-1 (25 m × 0.2 mm × 0.33 μm film thickness; Hewlett Packard, Avondale, PA) held at 75° for 1 min and increasing to 280° at a rate of 15°/min with helium as carrier gas at 130 kPa head pressure. The injection port temperature was 280°, and the detector line was set at 310°. Electron impact (70 eV) ionization and selective ion monitoring were used to quantify 1′-OHM at m/z 310, 4-OHM at m/z 398, and $^{15}N_3$ 1′-OHM at m/z 403. The retention times were 17.9 and 17.6 min for 1′-OHM and 4-OHM, respectively. Peak height ratios were used for quantification. Metabolite standard curves (2–100 ng) and quality controls were run with each set of samples. A baseline level of metabolite was seen even when HPLC-purified MDZ was injected directly onto the gas chromatography-mass spectrometry. To account for this, microsomal blanks (reaction mixture minus the microsomal protein) were run in parallel with each set of microsomal samples. The subsequent peak-to-height ratios were subtracted from the ratios of the sample metabolite formation determination. For the kidneys with the higher activities, the blank amounts accounted for <2% of the total peak-to-height ratio of formation. For the kidneys with lower activity, however, the blanks accounted for as much as 15–20% of detected metabolite. The quality controls fell within 10–17% of expected values for 1′-OHM, and the limit of detection was ~500 pg.

Immunoblotting. Kidney microsomal protein (0.6–100 μg) was loaded onto a 10% sodium dodecyl sulfate-polyacrylamide gel (16 × 20 cm/0.75 mm width) with a 4.5% stacking gel and electrophoresed for 3.5 hr at a constant current of 22 mA/gel, as described previously (5). HL-A and HL-E were used as controls. The samples were transferred to nitrocellulose with a 40% methanol/Tris/glycine blotting buffer at a constant current of 450 mA for 4 hr. The nitrocellulose blots were developed with a primary murine anti-human CYP3A4 antibody (also detects CYP3A5) in a 1:1000 dilution, followed by a

secondary murine antibody in a 1:2500 dilution with the enhanced chemiluminescence system (ECL, Amersham, Arlington Heights, IL). The anti-CYP3A4 antibody has been determined previously to be specific for CYP3A proteins under these conditions (5, 16). The rabbit anti-CYP3A5 primary antibody, previously determined to be selective in the detection of CYP3A5 (5), was used in a dilution of 1:500 and developed as described (*vide supra*). Relative density differences were determined with a model GS-670 Imaging Densitometer (Bio-Rad, Hercules, CA).

To take into account the nonlinearity and the variability of signal seen with the chemiluminescence system of development, immunoquantification was carried out with 39 ng of control HL-A in every second or third lane. In alternate lanes and in duplicate, a predetermined amount of each kidney microsomal sample was loaded onto the gel. Previous dilution blotting of each of the kidney samples was carried out to determine a protein amount that fell within the linear range of the film development capacity. To account for the variability of signal and linearity across the gel, ratios of the relative density of the kidney lane compared with the relative density of the control liver in the closest adjacent lane were measured and normalized to 1 μg of kidney microsomal protein. Duplicate values were averaged, and the experiment was repeated twice.

mRNA analysis. Frozen kidney samples (~150 μg) were placed into a denaturing solution (guanidinium thiocyanate, sodium lauryl sarcosinate, 2-mercaptoethanol), homogenized, and stored at −80°. The samples were thawed rapidly at 65°, and the following reagents were added sequentially: 30 μl of 2 M sodium acetate, pH 4.0, 300 μl of phenol saturated with diethylpyrocarbonate-treated water, and 60 μl of chloroform/isoamyl alcohol (49:1 v/v). This mixture underwent a series of differential centrifugations and denaturations to obtain an RNA pellet, which was then dissolved in diethylpyrocarbonate-treated water. The RNA content was measured spectrophotometrically as described previously (17).

cDNA was prepared according to previously described methods (16) with the following changes. Five microliters of reverse-transcriptase buffer (500 mM Tris, pH 8.3, 500 mM potassium chloride, 80 mM magnesium chloride, 100 mM dithiothreitol) and 6 μl of oligonucleotide dTT12–18 (Pharmacia, Piscataway, NJ) were added to 1 μg of kidney mRNA; the mixture was incubated to 65° for 3 min and then cooled slowly to 41°. One microliter of 25 mM dNTP and 1 μl of reverse transcriptase (Seikagaku, America Inc., Rockville, MD) were added, and the mixture was incubated at 41° for 1 hr, cooled, and stored at −80°.

For amplification, 1 μl of the prepared cDNA was added to 2.5 μl of 1 mM dNTP; 35 μl of PCR buffer (400 mM KCl, 0.1% gelatin); 2.5 μl of *Taq* polymerase (Perkin-Elmer, Norwalk, CT); 15.0 μl of diethylpyrocarbonate-treated water; 1.0 μl of magnesium chloride; 1.0 μl of antisense synthetic 30-mer 12.5 pM primer specific for CYP3A3, CYP3A4, CYP3A5, and CYP3A7; and 1.0 μl of 12.5 pM sense 30-mer oligonucleotide primer (16). Samples were amplified with a Perkin-Elmer DNA thermal cycler for 25–45 cycles using a 45-sec denaturation step (95° for 60 sec) and extension for 75 sec at 65° with annealing. The final extension was at 65° for 10 min, after which samples were cooled and stored at 4° until electrophoresis. The reaction mixture (20 μl) was loaded onto a 1.8% metaphor/ethidium gel, and electrophoresis was carried out under constant voltage conditions at 65 V for 60 min. Amplification of the appropriate segment was confirmed through the visualization of a band of appropriate length under UV light. All samples were run twice, with no difference noted. In addition, all samples that appeared to have a discrepancy between CYP3A4 mRNA and protein detection (i.e., the presence of protein but not mRNA, or vice versa) were run a third time, with no change in results (16).

Statistical analysis. To examine the enzyme activity and content of human kidney microsomes for a unimodal-versus-bimodal distribution within the sample population, the NTV procedure was used as described by Endrenyi and Patel (18). Confidence intervals were calculated according to conventional procedures.

Results

The CYP3A activity of human kidney microsomes was determined with MDZ, a well-known CYP3A4/5 substrate, through the measurement 1′-OHM formation. The dependence of MDZ hydroxylation rate on substrate concentration was examined for three kidneys over a range of 3.1–400 μM. The three kidneys exhibited maximum velocities of 9.4 (IUK 9), 181.0 (IUK 6), and 261.0 (IUK 11) pmol/hr/mg protein at substrate concentrations of 12.5–50 μM (Fig. 1). At higher substrate concentrations, metabolite formation rates declined in each case, suggesting that substrate inhibition or inactivation of the CYP3A was occurring (Fig. 1). In view of the complexity of the metabolite formation patterns, Michaelis-Menten constants were not estimated, and all subsequent activities were determined at a substrate concentration of 12.5 μM. The rate of 1′-OHM formation at 12.5 μM substrate concentration was determined for 27 kidney microsomal samples (Table 1 and Fig. 2) and examined for the potential presence of a nonunimodal distribution according to the NTV procedure as described previously (18).

Significantly negative NTV values (NTV <0.03) are con-

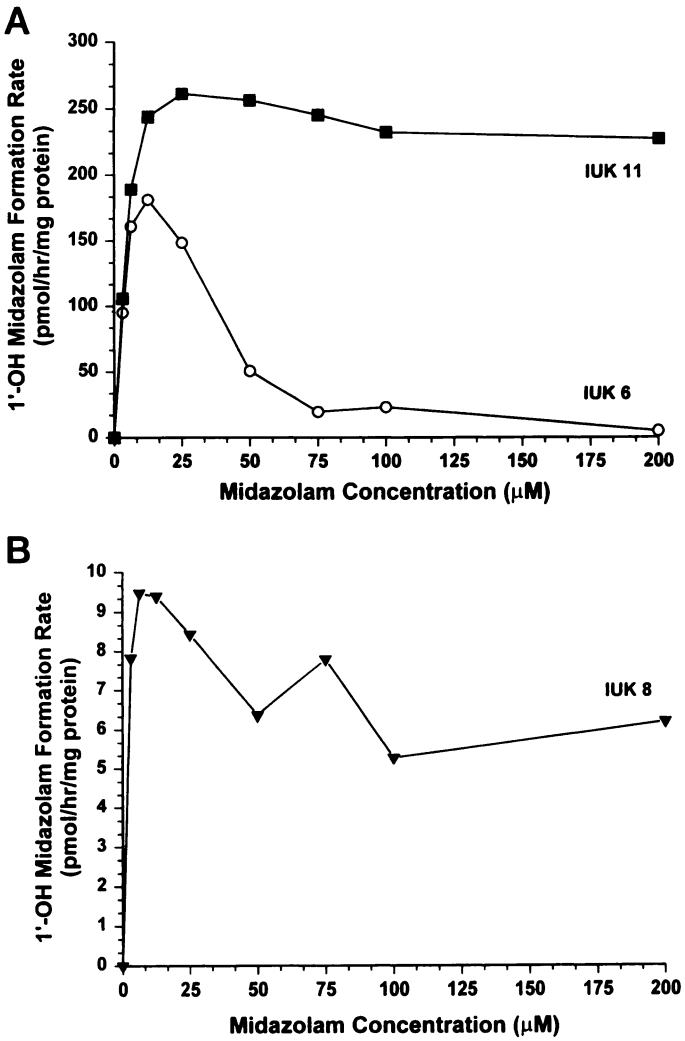

Fig. 1. A, Dependence of 1′-OHM formation rate on substrate concentration. Depicted are IUK 11 and IUK 6, which have relatively high activity. B, Dependence of 1′-OHM formation rate on substrate concentration. Depicted is IUK 8, which has relatively low activity.

TABLE 1

1′OHM formation rate, CYP3A protein content, and CYP3A mRNA content in human kidney

IUK No.	1′-OHM formation	CYP3A5 Protein	CYP3A5 mRNA	CYP3A4 Protein	CYP3A4 mRNA	Portion of kidney[a]	Portion of kidney[a]
	pmol/hr/mg protein					*microsomes*	*RNA*
1	4.6	+	+			Whole	Whole
2	4.8	+	+			Whole	Whole
3	1.5[b]	+	+			Whole	Whole
4	1.9	+	+	+		Whole	Whole
5	5.6	+	+		+	Whole	Whole
6	190.6	++++	+			Cortex	Medulla
7	7.0	+	+			Whole	Whole
8	3.3	+	+		+	Cortex	Medulla
9	169.5	++++	+		+	Cortex	Cortex
10	2.5	+	+	+	+	Whole	Whole
11	201.0	++++	+		+	Whole	Whole
12	ND	ND	+	ND	+	ND	Whole
13	9.4	+	+	+		Whole	Whole
14	8.5	+	+	+		Whole	Whole
15	9.5	+	+			Cortex	Medulla
16	13.3	+	+			Cortex	Cortex
17	ND	ND	+	ND		ND	Whole
18	10.9	+	+	+	+	Cortex	Cortex
19	21.9	+	ND		ND	Whole	ND
20	8.7	+	+	+		Cortex	Cortex
21	14.4	+	+	+	+	Medulla	Cortex
22	18.8	+	+	+	+	Cortex	Medulla
23	8.9	+	+	+		Cortex	Cortex
24	10.2	+	ND	+	ND	Cortex	ND
25	22.6	+	+	+	+	Cortex	Medulla
26	21.1	+	+	+		Cortex	Medulla
27	13.0	+	+	+	+	Whole	Whole
28	175.2	++++	+			Cortex	Cortex
29	11.7	+	+	+		Cortex	Cortex

ND, not determined.

[a] Whole includes portions of medulla and cortex; cortex includes portion of cortex only; and medulla includes portions of medulla only.

[b] 1.5 lowest limit of detection 500 pg/800-μl reaction volume.

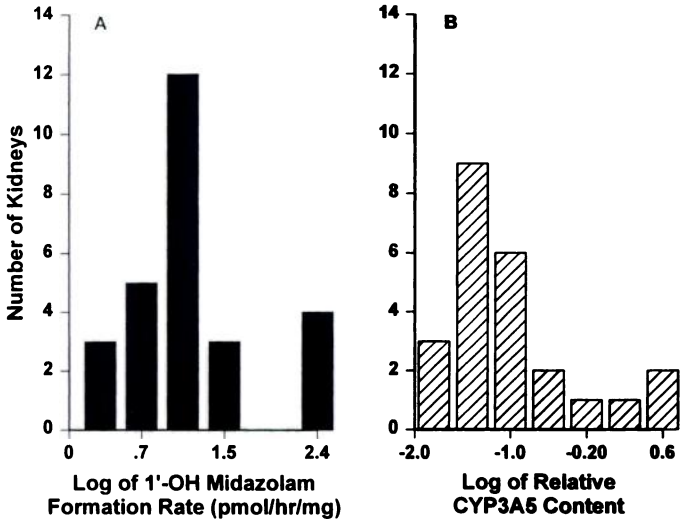

Fig. 2. A, Distribution of 1′-OHM formation rate (pmol/hr/mg) (27 samples). B, Immunoquantified CYP3A5 content (24 samples) in human kidney microsomes. Enzyme content is expressed as absorbance of kidney sample (normalized to 1 μg of microsomal protein) relative to liver (HL-A). The *x*-axis in both figures are numbered so that the labeled value represents the midpoint of the range of log values for a particular number of kidneys.

sidered diagnostic of distinct modes, and the minimum value of NTV corresponds to the antimode. The 1′-OHM formation rates exhibited a minimum NTV value of −0.08, corresponding to IUK 9 (Table 1). The latter is consistent with a bimodal distribution of catalytic activities in which the antimode corresponds to a 1′-OHM formation rate of 169.5 pmol/hr/mg (2.2 on log scale), suggesting that the four samples with the highest activity (IUK 6, 9, 11, and 28) constitute a distinct population (Table 1 and Fig. 2). The four high-activity samples had a mean formation rate (± standard deviation) of 184.0 ± 14.1 pmol/hr/mg microsomal protein compared with 10.1 ± 6.4 pmol/hr/mg for the remaining 23 samples. The high-activity group (four samples) had a mean formation rate that fell well outside the 99.9% confidence interval of the mean low-activity formation rate (23 samples), which ranged from 5.7 to 14.5 pmol/hr/mg.

In the four kidneys with the greatest activity, the formation of 4-OHM was also readily detected. For kidney samples 6, 9, 11, and 28, 4-OHM formation rates of 33.3, 38.1, 43.3, and 17.4 pmol/hr/mg, respectively, were obtained. Mean inhibition of IUK 6 and 28 was 53% and 57% when kidney microsomes were incubated with 100 μM triacetyloleandomycin and with 10 μl of inhibitory CYP3A antibody, respectively, as described in Materials and Methods.

The bimodal distribution of activity was not observed for either sulindac sulfide oxidation to *R*-sulindac sulfoxide or the methylhydroxylation of tolbutamide.[1] These are mediated by flavin-dependent monooxygenases and CYP2C8/9, respectively. The mean rate of *R*-sulindac sulfoxide formation (± standard deviation) was 333.0 ± 145.0 pmol/mg/min protein in the high activity kidney samples and 235.0 ± 97.2

[1] M. A. Hamman and S. D. Hall, unpublished observations.

pmol/min/mg in the low-activity kidney samples. The rates of hydroxytolbutamide formation (± standard deviation) were 0.4 ± 0.1 pmol/min/mg protein and 0.4 ± 0.4 pmol/min/mg of protein for the high- and low-activity samples, respectively. These two microsomal activities represent distinct enzymes from CYP3A and clearly do not exhibit the bimodal characteristics, as does the 1′-OHM formation rate.

With the use of murine monoclonal anti-CYP3A IgG, 27 kidney microsomal samples and liver samples HL-A and HL-E were examined for CYP3A content. All 27 kidney samples contained an immunochemically detected protein that comigrated with CYP3A5 protein. A fainter band that comigrated with the liver CYP3A4 band was found in 14 samples, which may represent a small amount of CYP3A4 but also may represent a breakdown product of CYP3A5 (Fig. 3). A third, lower-molecular-weight band was seen in selected kidney samples (Fig. 3, IUK 29) when large amounts of kidney microsomal protein were loaded. This band disappeared as smaller quantities of microsomal protein were loaded. This probably is not a CYP3A5 breakdown product, but it may represent a kidney-specific protein that cross-reacts with the CYP3A4 antibody. Specific anti-CYP3A5 antibody used as described in Materials and Methods (data not shown) detected protein that comigrated with CYP3A5 protein only in the kidneys with the highest relative activity and protein content, indicating a loss of sensitivity with the anti-CYP3A5 antibody purification process compared with the less-specific murine CYP3A antibody, which detects both CYP3A4 and CYP3A5.

The kidneys with the highest catalytic activity also had a ≥10-fold CYP3A5 content relative to the 23 remaining samples. The relative mean content (± standard deviation) of CYP3A5 expressed as absorbance of kidney sample (normalized to 1 μg of microsomal protein) relative to liver HL-A was 2.2 ± 1.0 for the kidneys with the high protein content (four samples) and 0.08 ± 0.08 for the kidneys with low protein content (20 samples). The high protein-content group (four samples) had a relative mean content that fell well outside the 99.9% confidence interval of the mean content of the group with the low protein content (20 samples), which ranged from 0.02 to 0.1. When the relative CYP3A5 protein content was compared with the ratio of 1′OHM formation in this bank of kidney microsomes, a high correlation coefficient was obtained (r^2 = 0.84; Fig. 4). This value may be falsely high due to the discontinuous data distribution. This is illustrated by the separate analysis of the low- and high-activity samples, which reveals no correlation between protein and activity data in the low-activity kidneys and r = 0.65 for the high-activity kidneys. It is, therefore, a possibility that some of the activity seen is not due to CYP3A5 or, more likely, that

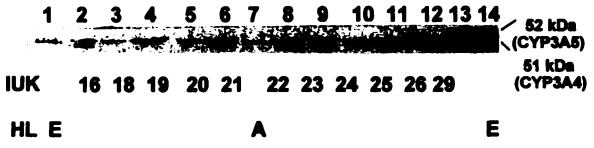

Fig. 3. CYP3A4 and CYP3A5 contents of human kidney microsomes were resolved with the use of sodium dodecyl sulfate-polyacrylamide gel electrophoresis (10%), transfered to nitrocellulose, and immunoblotted with murine monoclonal anti-CYP3A IgG. HL-E contains CYP3A4 and CYP3A5 (31 ng of microsomal protein); HL-A contains only CYP3A4 (39 ng). IUK lanes contain 100 μg of microsomal protein. *Top numbers*, lane of the gel; *bottom numbers*, kidney sample.

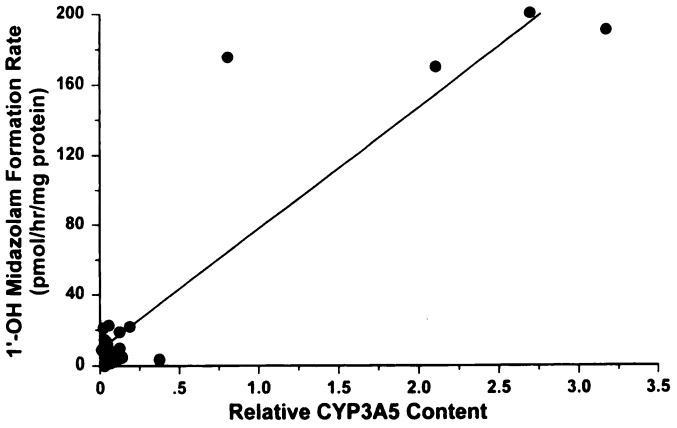

Fig. 4. Correlation of 1′-OHM formation rate (24 samples) and relative immunoquantified CYP3A5 content where r = 0.92 and r^2 = 0.84. Enzyme content is expressed as absorbance of kidney sample (normalized to 1 μg of microsomal protein) relative to HL-A.

this reflects a high degree of variability of response (in catalytic activity and immunodetection) near the lower limits of detection. As described above, the NTV procedure was also used to examine the distribution of relative CYP3A5 content in the bank of kidney microsomes (18). A NTV value of −0.06 corresponded to IUK 28, suggesting a bimodal distribution of CYP3A5 content and an antimode of 0.81 relative absorbance (−0.09 on log scale). Four samples (IUK 6, 11, 9, and 28) therefore constitute a distinct population with respect to both catalytic activity and relative CYP3A5 content (Table 1 and Fig. 2). It is important to note that there was no apparent relationship between catalytic activity and kidney donor characteristics, such as age, sex, renal function, significant past medical history, tumor size and characteristics, or drug therapy. Total content of CYP3A5/mg of kidney microsomal protein was 100-1000-fold less of than that CYP3A4 found in hepatic microsomal protein (Fig. 5). This corresponded to a ≥100-fold difference in ability for kidney versus hepatic microsomal protein to form 1′-OHM. For example, at 6.25 μM MDZ, a bank of 18 human liver microsomal samples had a mean activity (± standard deviation) (1′OHM formation) of 348.0 ± 334.0 pmol/min/mg protein (14) compared with the mean activity of the four kidneys with the highest activity (3.1 pmol/min/mg protein) and the 23 kidneys with the mean lowest activity (0.2 pmol/min/mg protein).

The mRNA expression was characterized with the use of DNA oligonucleotides specific for CYP3A3, CYP3A4, CYP3A5, and CYP3A7, as well as control oligonucleotides,

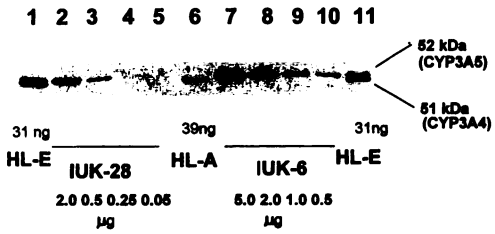

Fig. 5. Comparison of human liver and kidney microsomal protein contents of CYP3A4 and CYP3A5 with the use of Western blotting. Proteins were resolved through sodium dodecyl sulfate-polyacrylamide gel electrophoresis (10%), transfered to nitrocellulose, and immunoblotted with murine monoclonal anti-CYP3A IgG. HL-E contains CYP3A4 and CYP3A5 (31 ng of microsomal protein); HL-A contains only CYP3A4 (39 ng). IUK 28 and IUK 6 have relatively high CYP3A contents.

multidrug resistance-1 gene, and ubiquitin, with subsequent cDNA preparation and PCR amplification (Fig. 6). All 27 samples contained CYP3A5 message, which corresponded to the protein data obtained (Table 1). Only 25 of these had corresponding CYP3A protein contents determined due to a limited tissue supply of particular kidneys. Eleven of 27 (1 of which was IUK 12, for which no protein data are available) also contained message for CYP3A4 (Table 1). Seven of 10 samples containing CYP3A4 mRNA also had a band that comigrated in immunoblot analysis with CYP3A4. The remaining 3 samples that contained CYP3A4 and CYP3A5 mRNA had a single detectable 52-kDa band indicating the expression of CYP3A5 alone or the expression of CYP3A4 below the limit of detection. Also of note were seven kidneys that contained only the CYP3A5 message but expressed a protein that comigrated with the CYP3A4 in hepatic microsomes. It is possible that in these samples the detected band is a degradation product of CYP3A5. There was no obvious correlation between the source of microsomes, e.g., cortex or medulla, and the presence or absence of CYP3A4 message. Interestingly, one kidney contained mRNA corresponding to CYP3A7, the fetal form of CYP3A, but a 51.5-kDa protein band migrating in between the 51-kDa and the 52-kDa proteins was not identified in this kidney sample. CYP3A3 mRNA was not detected in any of the samples. The multidrug resistance sequence was determined to be a more consistent control and was detected in all kidney samples except IUK 6 and IUK 14, whereas ubiquitin was detected only sporadically.

Discussion

CYP3A4 is known to be a major drug-metabolizing enzyme in human liver (14) and gut (16) and is also known to be involved in the metabolism of endogenous steroids, such as cortisol, progesterone, and testosterone (19). Some renal CYPs, such as CYP2C and CYP4A, are relatively well characterized and are involved in generating arachidonic acid metabolites, which are vasoactive and alter renal tubular ion transport (20, 21). It is likely that one or more renal CYP3A enzymes also play a role in salt and water balance (8, 9).

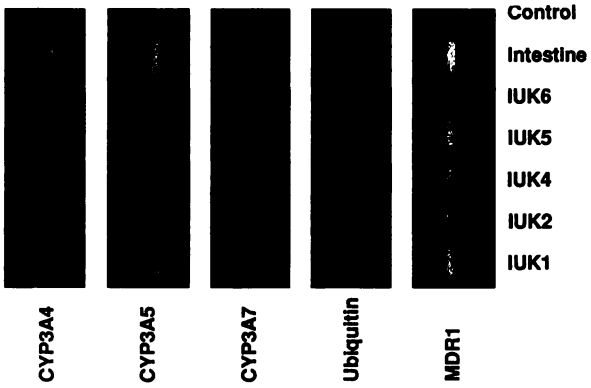

Fig. 6. PCR products obtained from cDNA samples prepared from the kidney samples with intestine run as control. Synthetic oligonucleotide primers complementary to hypervariable regions of the CYP3A cDNAs (described in Materials and Methods) were used to amplify fragments of CYP3A3, CYP3A4, CYP3A5, and CYP3A7 cDNA. Multidrug resistance-1 gene (*MDR1*) and ubiquitin cDNA were used as controls. These were then run on 1.8% metaphor/ethidium gel and visualized under UV light (described in previous methods).

CYP3A has been located in both areas of high-volume water and solute transport, such as the proximal tubule, and areas of fine tuning, such as the cortical collecting ducts (3). It is clear that CYP3A4 (4) and CYP3A5 (5) catalyze the conversion of cortisol to 6β-OHC and that several tissues are capable of effecting this biotransformation, including the liver, kidney, adrenal cortex, and gut. The relative contribution of these organs to total body cortisol hydroxylation, however, is unclear (16, 22). It is unlikely that the normal adrenal gland contributes significantly to the total production of 6β-OHC (22–24). Gut CYP3A may be capable of metabolizing cortisol to 6β-OHC, but probably only exogenously, orally administered cortisol has sufficiently high exposure to the luminal gut epithelium to provide a significant contribution to total urinary 6β-OHC excretion. Therefore, it has been generally accepted that the liver plays a major role in producing 6β-OHC in view of its high CYP3A4 content. The urinary 6β-OHC/cortisol ratio has been used as a marker of hepatic CYP3A activity (25) and is increased by typical CYP3A4 inducers, such as rifampin (26, 27). However, there is an absence of correlation between the urinary cortisol ratio and other indices of hepatic CYP3A, such as the erythromycin breath test, which suggests that organs other than the liver (the kidney in particular) may contribute to the overall urinary excretion of 6β-OHC (28, 29). The latter is consistent with the observation that during the anhepatic phase of liver transplantation, 6β-OHC/cortisol urinary ratios initially dropped, consistent with the half-life of cortisol (30), but plateaued for the final 90 min, during which the patient was without a liver (28). Therefore, this strongly suggests that in addition to the production of 6β-OHC by the liver, a portion is a nonhepatically derived and contributes substantially to the total amount of 6β-OHC recovered in the urine.

The significance of renal 6β-hydroxylation of corticosteroids in Na^+ transport has been illustrated with A_6 cultured toad renal epithelial cells, which respond the to additions of 6β-hydroxycorticosterone and 6β-OHC with a stimulation of transepithelial sodium transport via a unique type IV nuclear receptor (6, 7, 31). There also is evidence of a receptor of this type in mammals; rats treated with 6β-hydroxycorticosterone experienced sodium retention (32). An analogy to this in humans is that sodium retention produced by stress doses of cortisol cannot be completely reversed with mineralocorticoid and glucocorticoid antagonists, which are known to act at distinct receptor loci (2, 33).

In the current study, we characterized the CYP3A activity, protein, and mRNA content in human kidneys as a first step in understanding the potential physiological significance of this CYP subfamily in the kidney. The catalytic activity of renal CYP3A was quantified as the rate of formation of 1′-OHM, the primary human metabolite of MDZ (14). For kidneys with the highest activity, the rate of 1′-OHM formation (four samples; 184.0 ± 14.4 pmol/hr/mg or 3.1 pmol/min/mg microsomal protein at 12.5 μM MDZ) was substantially lower than that seen in hepatic microsomes (14 samples; 348.0 ± 334.0 pmol/min/mg at 6.25 μM and 495.0 ± 508.0 pmol/min/mg at 400 μM) (14). This substantial activity difference in catalytic activity corresponds to the 100-1000-fold difference in relative CYP3A protein content of hepatic versus kidney microsomes. The substantially lower CYP3A activity seen in the renal microsomal preparations would be consistent with a discrete localization of these enzymes in the

nephron (*vide supra*). In particular, areas with a high CYP3A content, such as the proximal tubule and cortical collecting ducts (3), represent a small fraction of total kidney protein, and therefore on a per-cell basis, these cells could contain a specific CYP3A content comparable to that of the hepatocyte.

It is important to point out that the predominant isoforms in the kidney and liver differ, which makes direct comparison of the individual isoforms (CYP3A4 and CYP3A5) in each organ difficult. Relative immunoquantified amounts of CYP3A4/5 have been previously determined to be 3:1 in human liver in those that express both isoforms (5). Therefore, 75% of the immunodetected CYP3A in the liver represents CYP3A4. It is not possible to strictly quantify CYP3A4 in the human kidney. The CYP3A4 is neither well resolved or quantifiable by available methods. It is clear, however, that CYP3A5 is the predominant CYP3A in the kidney; it probably represents >75% of the total CYP3A content in the human kidney. Therefore, when comparing total CYP3A content/activity of liver to kidney, hepatic CYP3A4 versus renal CYP3A5 represents a comparison of at least 75% of the total CYP3A content in each organ.

The maximum velocity of MDZ hydroxylation observed in the study kidney microsomes does not represent a true V_{max} because significant substrate inhibition was seen at substrate concentrations of >12.5–25 μM (Fig. 1). This behavior has also been noted in hepatic microsomes with MDZ as a substrate (14, 34), but to a variable and generally lesser degree. Of note, however, is that in our study, purified, reconstituted CYP3A5 and CYP3A4 exhibit simple hyperbolic kinetics with no evidence of substrate inhibition (14). Substrate inhibition seems to be more substantial and variable in kidney than in liver microsomes, which may reflect a different milieu of lipids and proteins found in kidney versus liver microsomes. Whether this substrate inhibition represents a tissue-selective, allosterically mediated regulation of CYP3A or inactivation of the active site by the substrate is unclear. The latter is unlikely given that the same inhibition pattern is observed in those kidneys with very low rates of metabolism as well as those with high activity and that metabolite formation was linear for 2 hr. If the assumption is made that the rate of 1′-hydroxylation at 12.5–25 μM approximates V_{max} in kidney microsomes, then the K_m would be ~6.25 μM, which is consistent with the 2–12 μM range for K_m noted in hepatic microsomes (14).

CYP3A4 is universally expressed in human liver, whereas CYP3A5 is expressed in only ~20% of individuals (5). In contrast, Schuetz *et al.* (2) noted that in a small number of human kidney microsomal samples, CYP3A5 was highly expressed in five of seven samples, whereas CYP3A4 was expressed in only 14% of samples. Our data confirm this general pattern of expression, but importantly, we demonstrated that CYP3A5 and the corresponding mRNA were detected in all 25 kidneys examined (Table 1). In addition, CYP3A4 mRNA was detectable in 11 of 27 kidneys (40%), and 70% of these revealed a protein band that comigrated with CYP3A4 on immunoblot. This general concordance between our mRNA and protein data indicates that the protein bands that we identified as CYP3A4 and CYP3A5 in kidney microsomes are highly similar, if not identical to, those previously characterized in human liver. Schuetz *et al.* also provided preliminary evidence that renal cortex contained 1.5 times the amount of CYP found in the medulla. We found no consistent differences in CYP3A5 content, activity, or mRNA content among these regions. Given the detection of CYP3A proteins in the proximal tubules, cortical collecting ducts, thin limb of Henle, and the cells lining the renal pelvis, a uniform distribution of CYP3A5 throughout the cortex and medulla is not unexpected (3).

We previously demonstrated that unlike most substrates, MDZ 1′-hydroxylation is catalyzed more efficiently by purified, reconstituted CYP3A5 than by CYP3A4; the 1′-OHM/4-OHM formation ratios were 10.3 and 3.6, respectively, at a substrate concentration of 12.5 μM (14). The rate of formation of 4-OHM by kidney microsomes was often at or even below the level of accurate quantification, especially in the kidneys that exhibited low 1′-OHM formation. However, for the four kidneys with high activity, the 4-OHM formation was well within detection limits (mean ± standard deviation of 33.0 ± 11.2 pmol/hr/mg protein, four samples), and the 1′-OHM/4-OHM formation ratios for these samples had a mean ± standard deviation of 6.3 ± 5.6, which is similar to that seen with purified CYP3A5. The metabolite formation ratios together with the immunoquantified enzyme levels and the lack of detectable CYP3A4 in most samples suggest that CYP3A5 is primarily responsible for the hydroxylation of MDZ in the human kidney. The significance of the variable expression of CYP3A4 in human kidneys is unclear given its low level of expression relative to CYP3A5.

Clearly, further studies are indicated to determine the mechanism and physiological relevance of the organ-specific expression of CYP3A enzymes. To date, there is no evidence to suggest that CYP3A5 is inducible by well known CYP3A4 inducers such as rifampin and dexamethasone (5, 35). The mechanism underlying the apparently bimodal distribution of immunoquantified CYP3A5 and 1′-OHM formation rate in human kidneys, therefore, remains to be established. If CYP3A5 is involved in the regulation of renal hemodynamics and ion homeostasis, possibly through its intrarenal conversion of cortisol to 6β-OHC, then intrarenal or systemic changes in hemodynamics and volume status, along with the presence or absence of intrinsic renal disease, may act as physiological regulators of renal CYP3A5 expression and catalytic activity. In the bank of kidney microsomes that were collected, however, no clear patient characteristics, such as age, sex, renal function (the majority of these individuals had normal renal function by serum creatinine), significant past medical history (e.g., hypertension, heart disease, liver disease, vascular disease, renal disease other than the tumor), tumor size and involvement, or drug therapy, were associated with those individuals who had high activity. It must be stressed that as a rule, most of these individuals were Caucasian and "healthy" except for the presence of the tumor. Few had significant preexisting medical conditions. This is likely why no detectable relationship existed between renal CYP3A activity/expression and pathology, including the existence of hypertension. In addition, the number of individuals may be too small to reveal a difference.

An alternative possibility to explain the bimodality of activity and expression is that there is an organ-specific regulatory polymorphism by which a specific gene promoter region or regions are controlled by the presence or absence of regulatory kidney-specific proteins. Accordingly, the level of renal CYP3A5 expression is intrinsically controlled at the organ level by poorly understood factors. This could have

clinically significant implications if these individuals with high intrarenal CYP3A5 experience increased conversion of cortisol to 6β-OHC and thereby tend to develop salt-sensitive hypertension.

A third possibility to explain the two populations of activities/expression seen is that those with high renal CYP3A5 activity (16%) correspond with the 20–25% of individuals who express CYP3A5 in the liver. However, because regulatory factors, organ function, and the role of CYP differ greatly in the kidney and liver, the expression of these CYP3A5 in each of these organs is not likely to be directly related to one another.

In conclusion, CYP3A is found in discrete portions of the nephron that are associated with both high volume and fine tuning of water and solute transport. The predominant CYP3A in the kidney is CYP3A5, which exhibits an expression pattern suggesting bimodality and is primarily responsible for the hydroxylation MDZ. It is unknown whether the elevated activity and protein levels in the four samples represent a small number of induced individuals or an organ-specific genetic regulation.

References

1. McGiff, J. C., C. P. Quilley, and M. A. Carroll. The contribution of cytochrome P450-dependent arachidonate metabolites to integrated renal function. *Steroids* **58:**573–579 (1993).
2. Schuetz, E. G., J. D. Schuetz, W. L. Grogan, A. Naray, F. Toth, G. F. Toth, J. Raucy, P. Guzelian, K. Gionela, and C. O. Watlington. Expression of cytochrome P450 3A in amphibian, rat, and human kidney. *Arch. Biochem. Biophys.* **294:**206–214 (1992).
3. Leggat, J. E., K. J. Johnson, J. C. Kolars, P. Schmiedlin-Ren, P. B. Watkins, and A. B. Leightman. Immunohistochemical localization of cytochrome P4503A in normal and neoplastic kidney and urinary bladder epithelium. *J. Am Soc. Nephrol.* **5:** 786 (1994).
4. Waxman, D. J., C. Attisano, P. F. Guengerich, and D. P. Lapenson. Human liver microsomal steroid metabolism: identification of the major microsomal steroid 6β-hydroxylase cytochrome P450 enzyme. *Arch. Biochem. Biophys.* **263:**242–436 (1988).
5. Wrighton, S. A., W. R. Brian, M. Sari, M. Iwasaki, F. P. Guengerich, J. L. Raucy, D. T. Molowa, and M. VandenBranden. Studies on the expression and metabolic capabilities of human liver cytochromes P450 3A5 (HLP 3). *Mol. Pharmacol.* **38:**207–213 (1990).
6. Duncan, R. L., W. M. Grogan, L. B. Kramer, and C. O. Watlington. Corticosterones' metabolite is an agonist for sodium transport stimulation in A6 cells. *Am. J. Physiol.* **225:**F736–F748 (1988).
7. Grogan, W. M., V. M. Phillips, E. G. Schuetz, P. S. Guzelian, and C. O. Watlington. Corticosterone 6β-hydroxylase in A6 epithelia: a steroid inducible cytochrome P450. *Am. J. Physiol.* **258:**C480–C488 (1990).
8. Ghosh, S., W. M. Grogan, A. Basu, and C. O. Watlington. Renal corticosterone 6β-hydroxylase in the spontaneously hypertensive rat. *Biochim. Biophys. Acta* **1182:**152–156 (1993).
9. Watlington, C. O., L. B. Kramer, E. G. Schuetz, W. Zilai, W. M. Grogan, P. Guzelian, G. Gizek, and A. Schoolwerth. Corticosterone 6β-hydroxylation correlates with blood pressure in spontaneously hypertensive rats. *Am. J. Physiol.* **262:**F927–F931 (1992).
10. Levere, R. D., P. Martasek, B. Escalente, M. L. Schwartzman, and N. G. Abraham. Effect of homoarginate administration on blood pressure in spontaneously hypertensive rats. *J. Clin. Invest.* **86:**213–219 (1990).
11. Sacerdoti, D. B., B. Escalente, N. G. Abraham, J. C. McGiff, R. D. Levere, and M. L. Schwartzman. Treatment with tin prevents the development of hypertension in the spontaneously hypertensive rat. *Science (Washington D. C.)* **243:**388–390 (1989).
12. Funae, Y., R. Seo, and S. Imaoka. Multiple forms of cytochrome P450 from microsomes of rat liver, kidney lung by HPLC. *Biochem. Intern.* **11:**523–531 (1985).
13. Lowry, O. H., N. H. Rosenbrough, A. L. Farr, and F. J. Randall. Protein measurement with Folin phenol reagent. *J. Biol. Chem.* **193:**265–275 (1951).
14. Gorski, J. C., S. D. Hall, D. R. Jones, M. VandenBranden, and R. Wrighton. Regioselective biotransformation of midazolam by members of the human CYP3A subfamily. *Biochem. Pharmacol.* **47:**1643–1653 (1994).
15. Gorski, J. C., D. R. Jones, S. A. Wrighton, and S. D. Hall. Characterization of dextromethorophan N-demethylation by human liver microsomes. *Biochem. Pharmacol.* **48:**173–182 (1994).
16. Kolars, J. C., K. S. Lown, P. Schmiedlin-Ren, M. Ghosh, C. Fang, S. A. Wrighton, R. M. Merion, and P. B. Watkins. CYP3A gene expression in human gut epithelium. *Pharmacogenetics* **4:**247–259 (1994).
17. Chomczynski, P., and N. Sacchi. Single-step method of RNA isolation by acid guanidinium thiocyanate-phenol-chloroform extraction. *Anal. Biochem.* **162:**156–159 (1987).
18. Endrenyi, L., and M. Patel. A new sensitive graphical method for detecting deviations from the normal distribution of drug responses: the NTV plot. *Br. J. Clin. Pharmacol.* **32:**159–166 (1991).
19. Buters, J. T., K. R. Korzekwa, K. L. Kunze, Y. Omata, P. Hardwick, and F. J. Gonzalez. cDNA-directed expression of human cytochrome P450 using baculovirus. *Drug Metab. Dispos.* **22:**688–692 (1994).
20. Schwartzman, M. L., P. Martasek, A. R. Rios, R. D. Levere, K. Solangi, A. L. Goodman, and N. G. Abraham. Cytochrome P450-dependent arachidonic acid metabolism in human kidney. *Kidney Int.* **37:**94–99 (1990).
21. Imig, J. D., A. P. Zou, P. O. DeMontellano, Z. Sui, and R. J. Roman. Cytochrome p-450 inhibitors alter afferent arteriolar responses to elevations in pressure. *Am. J. Physiol.* **266:**H1879–H1885 (1994).
22. Lipman, M. M., F. H. Katz, and J. W. Jailer. An alternative pathway for cortisol metabolism: 6β-hydroxycortisol production by human tissue slices. *J. Clin. Endocrinol. Metab.* **22:**268–272 (1962).
23. Jenkins, J. S. Metabolism of cortisol by the human adrenal cortex *in vitro*. *J. Clin. Endocrinol. Metab.* **25:**649–654 (1965).
24. Katz, F. H., M. M. Lipman, A. G. Franz, and J. W. Jailer. The physiologic significance of 6β-hydroxycortisol in human corticoid metabolism. *J. Clin. Endocrinol.* **22:**71–77 (1962).
25. Dienvenu, T., E. Rey, G. Pons, P. D'Athis, and G. Olive. A simple noninvasive procedure for the investigation of cytochrome P450 IIIA dependent enzymes in humans. *Int. J. Clin. Pharmacol. Ther. Toxicol.* **29:**441–445 (1991).
26. Watkins, P. B., S. A. Wrighton, E. G. Scheutz, D. T. Molowa, and P. S. Guzelian. Identification of glucocorticoid inducible CYP450 in intestinal mucosa of rats and man. *J. Clin Invest.* **80:**1029–1036 (1987).
27. Ged, C., J. Rouillon, L. Pichard, J. Combalbert, N. Bressot, P. Bories, H. Michel, P. Beaune, and P. Maurel. The increase in urinary excretion of 6β-hydroxycortisol as a marker of human hepatic cytochrome P450IIIA induction. *Br. J. Clin. Pharmacol.* **28:**373–387 (1989).
28. Watkins, P. B., D. K. Turgeon, P. Saenger, K. Lown, J. Kolars, T. Hamilton, K. Fishman, P. Guzelian, and J. J. Voorhees. Comparison of urinary 6β-hydroxycortisol and the erythromycin breath test as measures of hepatic P450IIIA (CYP3A) activity. *Clin. Pharmacol. Ther.* **52:**265–273 (1992).
29. Kinirons, M. T., D. O'Shea, T. E. Downing, A. T. Fitzwilliam, L. Joellenbeck, J. D. Groopman, G. R. Wilkinson, and A. J. Wood. Absence of correlations among three putative *in vivo* probes of human cytochrome P4503A activity in young healthy men. *Clin. Pharmacol. Ther.* **54:**621–629 (1993).
30. Kishida, S., and D. Fukushima. Radioimmunoassay of 6β-hydroxycortisol in plasma and urine. *Steroids* **30:**741–740 (1977).
31. Perkins, F. M., and J. S. Handler. Transport properties of toad kidney epithelia in culture. *Am. J. Physiol.* **241:**C154–C159 (1981).
32. Watlington, C. O., J. Atkins, J. McNeil, W. Grogan, and J. Johnson. Corticosterone is converted to 6β-hydroxycorticosterone in rat: effects of the metabolite on urinary electrolyte excretion. *J. Steroid Biochem.* **31:** 947–954 (1988).
33. Clore, J. N., H. Estep, H. Ross-Clunis, and C. O. Watlington. Adrenocorticotropin and cortisol induced changes in urinary sodium and potassium excretion in man: effects of spironolactone and RU486. *J. Clin. Endocrinol. Metab.* **67:**824–831 (1988).
34. Kronbach, T., D. Mathys, M. Umeno, F. Gonzolez, and U. Meyer. Oxidation of midazolam and triazolam by human liver cytochrome P450 IIIA. *Mol. Pharmacol.* **38:**89–96 (1990).
35. Schuetz, E. G., J. D. Schuetz, S. C. Strom, M. T. Thompson, R. A. Fisher, D. T. Molowa, D. Li, and P. S. Guzelian. Regulation of human liver cytochrome P450 3A in primary and continuous culture of human hepatocytes. *Hepatology* **18:**1254–1262 (1993).

Send reprint requests to: Dr. B. D. Haehner, Clinical Pharmacology, Wishard Memorial Hospital, 1001 West 10th Street, Indianapolis, IN 46202. E-mail: barbarah@medwish.dmed.lupul.edu